Osteoarthritis and Cartilage 33 (2025) 330–340

Osteoarthritis and Cartilage

MicroRNA signature for early prediction of knee osteoarthritis structural progression using integrated machine and deep learning approaches

Afshin Jamshidi # [1], Osvaldo Espin-Garcia † ‡ § [2], Thomas G. Wilson ¶ [3], Ian Loveless ¶ [4], Jean-Pierre Pelletier # [5], Johanne Martel-Pelletier # * [6] [7], Shabana Amanda Ali ¶ ‖ [7] [8]

Osteoarthritis Research Unit, University of Montreal Hospital Research Centre (CRCHUM), Montreal, Canada
† *Department of Biostatistics, Schroeder Arthritis Institute and Krembil Research Institute, University Health Network, Toronto, Canada*
‡ *Dalla Lana School of Public Health and Department of Statistical Sciences, University of Toronto, Toronto, Canada*
§ *Department of Epidemiology and Biostatistics, University of Western Ontario, London, Canada, Toronto, Canada*
¶ *Henry Ford Health + Michigan State University Health Sciences, Detroit, USA*
‖ *Center for Molecular Medicine and Genetics, Wayne State University, Detroit, USA*

ARTICLE INFO

Article history:
Received 3 July 2024
Accepted 12 November 2024

Keywords:
Prognostic prediction model
Machine/deep learning
MicroRNA
Biomarkers
Osteoarthritis
Knee structural progression

SUMMARY

Objective: Conventional methodologies are ineffective in predicting the rapid progression of knee osteoarthritis (OA). MicroRNAs (miRNAs) show promise as biomarkers for patient stratification. We aimed to develop a miRNA prognosis model for identifying knee OA structural progressors/non-progressors using integrated machine/deep learning tools.
Methods: Baseline serum miRNAs from Osteoarthritis Initiative (OAI) participants were isolated and sequenced. Participants were categorized based on their likelihood of knee structural progression/non-progression using magnetic resonance imaging and X-ray data. For prediction model development, 152 OAI participants (91 progressors, 61 non-progressors) were used. MiRNA features were reduced through VarClusHi clustering. Key miRNAs and OA determinants (age, sex, body mass index, race) were identified using seven machine learning tools. The final prediction model was developed using advanced machine/deep learning techniques. Model performance was assessed with area under the curve (AUC) (95% confidence intervals) and accuracy. Monte Carlo cross-validation ensured robustness. Model validation used 30 OAI baseline plasma samples from an independent set of participants (14 progressors, 16 non-progressors).
Results: Feature clustering selected 107 miRNAs. Elastic Net was chosen for feature selection. An optimized prediction model based on an Artificial Neural Network comprising age and four miRNAs (hsa-miR-556-3p, hsa-miR-3157-5p, hsa-miR-200a-5p, hsa-miR-141-3p) exhibited excellent performance (AUC, 0.94 [0.89, 0.97]; accuracy, 0.84 [0.77, 0.89]). Model validation performance (AUC, 0.81 [0.63, 0.92]; accuracy, 0.83 [0.66, 0.93]) demonstrated the potential for generalization.
Conclusion: This study introduces a novel miRNA prognosis model for knee OA patients at risk of structural progression. It requires five baseline features, demonstrates excellent performance, is validated with an independent set, and holds promise for future personalized therapeutic monitoring.

* Correspondence to: Osteoarthritis Research Unit, University of Montreal Hospital Research Centre (CRCHUM), 900 Saint-Denis, R11.412B, Montreal, Quebec H2X 0A9, Canada.
E-mail addresses: afshin.jamshidi2@mcgill.ca (A. Jamshidi), oespinga@uwo.ca (O. Espin-Garcia), twilso20@hfhs.org (T.G. Wilson), ilovele1@hfhs.org (I. Loveless), dr@jppelletier.ca (J.-P. Pelletier), jm@martelpelletier.ca (J. Martel-Pelletier), sali14@hfhs.org (S.A. Ali).
[1] https://orcid.org/0009-0003-0190-2364
[2] https://orcid.org/0000-0003-2052-2626
[3] https://orcid.org/0000-0003-3416-5498
[4] https://orcid.org/0000-0003-4645-6559
[5] https://orcid.org/0000-0001-9930-6453
[6] https://orcid.org/0000-0003-2618-383X
[7] Both JMP and SAA are senior authors.
[8] https://orcid.org/0000-0002-4339-9467

https://doi.org/10.1016/j.joca.2024.11.008

Introduction

Knee osteoarthritis (OA) is the most disabling musculoskeletal condition, constituting a leading cause of long-term work incapacity and frequent visits to primary care doctors. Existing treatments for OA primarily alleviate symptoms without addressing structural changes in the joint. Therefore, preventing development or attenuating progression in early OA is a priority for developing new interventions. Unfortunately, conventional methodologies are ineffective in prognosticating patients whose disease will progress rapidly.

The challenges faced in discovering reliable biomarkers for early prediction of knee OA structural progression include the heterogeneity of disease development and the lack of methodologies enabling accurate classification of OA patients. As such, finding minimally invasive biomarkers to classify OA patients into subgroups centered on structural progression phenotypes is expected to support disease management. In addition, biomarkers are anticipated to support the development of OA therapeutics in the form of disease-modifying OA drugs (DMOADs), as one hurdle in clinical trial recruitment is the early detection of participants at risk for rapid structural progression of the disease.

Previous biomarker studies have typically defined knee OA progression based on radiography and/or symptoms. However, radiography alone is not sensitive to early knee structure alterations and their changes over time.[1] Additionally, OA symptoms lack a direct correlation with structural disease progression.[2] In contrast, magnetic resonance imaging (MRI) is very sensitive and effective at detecting early knee structural changes and tracking their progression over time, often identifying alterations before they appear with other imaging modalities.[3] Demonstrating this, an algorithm developed by our group showed that five features as inputs, three from MRI and two from radiography, could accurately predict knee OA progressors.[4] However, since MRI is not widely used in clinical settings for knee OA and this methodology could be costly, there remains a need for minimally invasive and cost-effective biochemical markers for knee OA progression. Therefore, circulating biochemical markers offer a suitable option.

Representing a promising new class of circulating biomarkers, microRNAs (miRNAs) are small non-coding RNA segments (~22 nucleotides) that are relatively stable and specific to various disease states.[5] In the context of OA, miRNAs have been shown to regulate joint tissue development, homeostasis, inflammation, cartilage degeneration, autophagy, and apoptosis, among other processes.[6,7]

While several studies have explored circulating miRNAs as potential biomarkers of OA,[8] only a handful of studies used sequencing, which is the current gold-standard approach for miRNA profiling. Of those studies, only one focused on OA progression, identifying four members of the miR-320 family linked to rapid progression of radiographic knee OA.[9] However, in this previous study, the characterization of the fast-progressing phenotype was based on radiography only, which, as noted above, is less sensitive than MRI for early prognosis. To fill this gap, the main objective of the present study was to identify a miRNA signature that predicts, at an early stage, individuals at risk of structurally progressive knee OA. We hypothesized that a prediction model with excellent performance could be developed and validated by defining structural progressors using both MRI and radiography[4] and applying machine and/or deep learning approaches to miRNA-sequencing data.

Methods

Study population

All participants were from the Osteoarthritis Initiative (OAI) cohort.[10] The training and testing cohorts used to develop the model comprised 152 baseline serum samples from the Incidence and Progression OAI subcohorts.

For the model validation, we used an independent set (compared to the modeling dataset) of 30 baseline plasma OAI samples obtained from an existing dataset from the OAI Gene Expression Omnibus database (GEO accession number GSE183188).[9] The relative global miRNA expression patterns between plasma and serum have been previously shown to be correlated.[11]

More details about the OAI cohort are available at https://nda.nih.gov/oai.

Sample size

The post hoc sample size was determined using a method specifically designed for studies involving the area under the receiver operating characteristic (AUROC) curve.[12] It is particularly suitable for our study because our outcome is binary (progressor vs. non-progressor), and our predictors are continuous (miRNA features).

The calculations were performed as follows:

- Calculate Q1 and Q2 using the formulae: $Q1 = \theta/(2-\theta) = 0.9048$; $Q2 = 2\theta^2/(1+\theta) = 0.9256$;
- Calculate the standard normal deviate for α ($Z\alpha$) = 1.9600;
- Calculate the Standard Error goal (SE goal) = $W/2Z\alpha = 0.031888$;
- Calculate $a = P(1-P)(\text{SE goal})^2 = 0.000244$;
- Calculate $b = -(P(Q1-Q2) + Q2 - \theta^2) = -0.0106$;
- Calculate $c = Q1 + Q2 - \theta - \theta^2 = -0.0221$.

The values in the formulae were derived as follows:

- θ (expected AUROC) was set to 0.95, based on prior estimates of model performance.
- P (proportion of the sample having the disease) was set to 0.6, reflecting the prevalence of the condition in our sample.
- W (width of the confidence interval) was chosen as 0.125, based on the desired precision.
- Confidence level (CI) was set at 95% for the calculations.

All the analyses were done using an online sample size calculator for designing clinical research (https://sample-size.net/sample-size-ci-for-auroc/). Q1 adjusts for the skewness of the ROC curve, while Q2 accounts for its overall shape, with θ representing the expected AUROC value.

MiRNA sequencing

Among high-throughput profiling techniques, miRNA sequencing is considered the gold-standard approach and offers unbiased quantification of miRNAs within a sample.[13] We followed customized methods for miRNA sequencing as previously described.[14]

Briefly, frozen aliquots of serum (n=152) samples collected at baseline were obtained from the OAI and stored at −80 °C until use. RNA was isolated from 200 µL using the miRNeasy Serum/Plasma Advanced kit (QIAGEN), and miRNA libraries were created using the QIAseq miRNA Library kit (QIAGEN). The quality of the libraries was evaluated with an Agilent TapeStation (D1000). Sequencing was performed on an Illumina MiSeq system utilizing a single-end 76-base read protocol.

As mentioned above, raw sequencing data for the independent validation plasma samples (n=30) were obtained from an existing GEO dataset. RNA isolation, miRNA library preparation and sequencing were performed using a similar pipeline to the one described above for serum samples.[9]

Analysis of miRNA-sequencing data

We followed a customized miRNA-sequencing analysis pipeline optimized for miRNA biomarker discovery.[15] Briefly, for serum and plasma samples, demultiplexing of.bcl files and conversion into Fastq files were performed to align the sequencing data and generate counts. Unique molecular identifiers were extracted, and reads were trimmed to select sequences between 18 and 30 bp. Two rounds of read alignment were carried out, first against mature miRNA sequences from the miRBase v22.1 database, followed by a second round against the human reference genome (vGRCh38), and miRNA counts from each alignment round were combined. Low-count miRNAs were filtered out to include only those with at least ten counts per million in two or more samples. The average mapped reads per sample for the serum modeling cohort was 915,000 ± 400,000, and 456 miRNAs were selected following low-count filtering.

Since serum and plasma samples were sequenced separately, we compared miRNA levels across these sample types. Using paired serum and plasma samples from nine OAI participants, Pearson correlation analysis revealed a very good correlation (Supplementary Fig. S1), suggesting that miRNA levels are comparable across these two biofluids.

Workflow for prioritizing the features

We undertook a stepwise approach to prioritizing miRNAs from the sequencing data (Fig. 1). The first step included labeling the 152 participants into progressors or non-progressors. Next, unsupervised dimensionality reduction was performed to identify the most informative miRNAs within the initial set of 456. This is an essential step, as high multicollinearity might lead machine learning to overfitting. Then, to identify the top miRNAs along with four OA risk

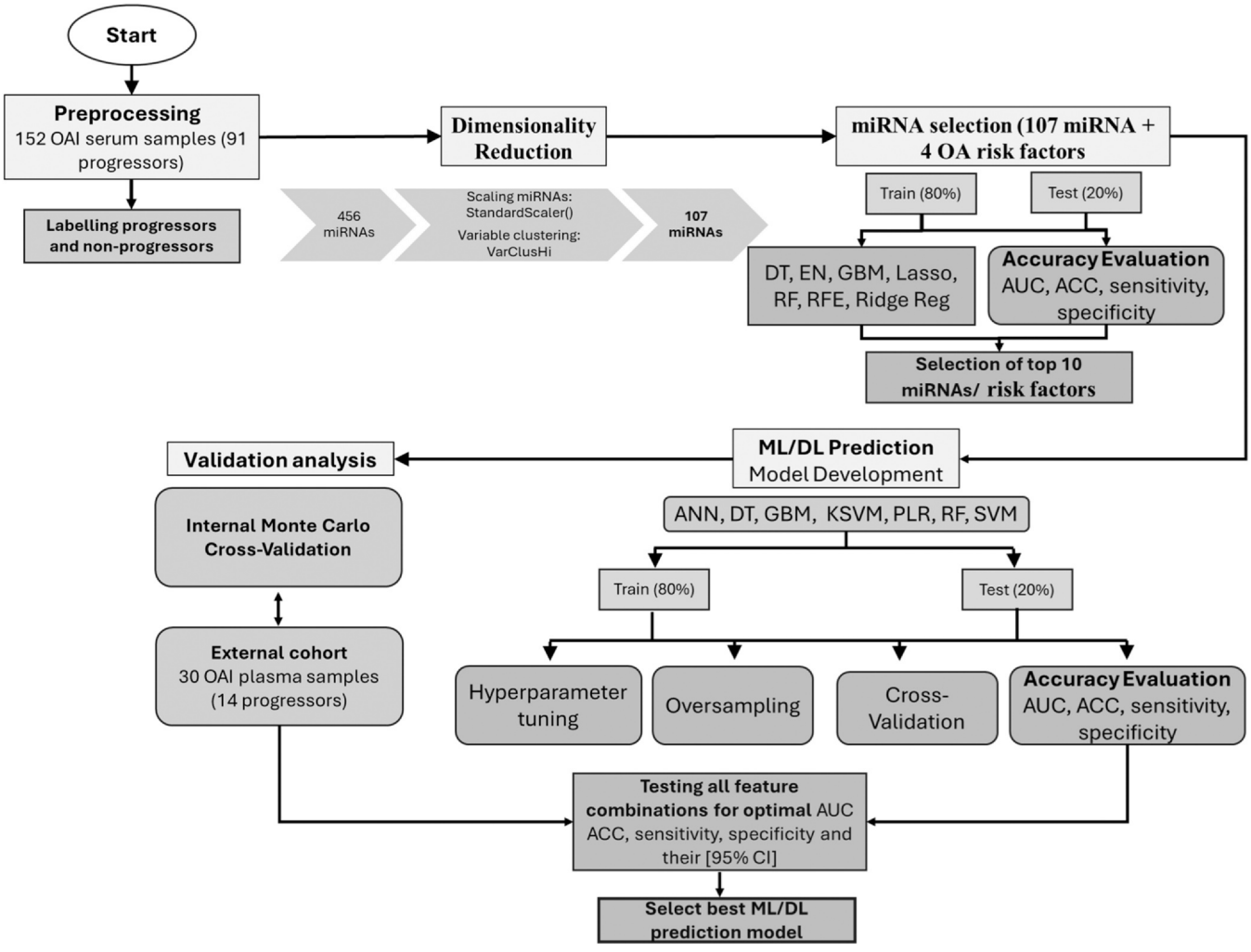

Fig. 1

Osteoarthritis and Cartilage

Workflow of the methodology for prioritizing the most relevant microRNAs/risk factors to discriminate participants into OA structural progressors/non-progressors. ANN, artificial neural network; ACC, accuracy; AUC [95% CI], area under the curve [95% confidence interval]; DL, deep learning; DT, Decision Tree; EN, Elastic Net; GBM, Gradient Boosting Machine; KSVM, Kernel Support Vector Machine; Lasso, Least Absolute Shrinkage and Selection Operator; ML, machine learning; miRNA, microRNA; OAI, Osteoarthritis Initiative; PLR, Penalized Logistic Regression; RF, Random Forest; RFE, Recursive Feature Elimination; Ridge Reg, Ridge Regression; SVM, Support Vector Machine; VarClusHi, a python package for feature clustering.

factors – including age, sex, body mass index (BMI), and race – predictive of knee OA structural progression, we first identified the best machine-learning model among seven and then classified the features. The output was the labeling of participants as progressors/non-progressors.[4] The participants were then separated randomly into 80% for the training dataset and the remaining 20% for testing. Further, seven machine/deep learning models were assessed with training and test datasets to identify the most effective miRNAs and risk factors. For each model, hyperparameter tuning, oversampling, and fivefold cross-validation with five repetitions were carried out, and the performance was evaluated with several metrics such as area under the curve (AUC) [95% confidence interval (CI)] using the Agresti-Coull interval[16] for the modeling cohort and the Wilson score interval[17] for the validation cohort in all feature selection and prediction model analyses, along with accuracy, sensitivity, and specificity with their [95% CI] for all models. A two-step validation was conducted with the final model to confirm its generalizability: i) an internal validation performed with Monte Carlo cross-validation[18] with 100 simulations and ii) a reproducibility analysis with an additional OAI dataset (independent to the one used for model development) of 30 plasma samples.

Labeling structural progressors and non-progressors

To define the progressor/non-progressor outcome for our study, we applied a classification approach based on our previously published methodology[4] also described in[19] This method was chosen because in addition to X-rays, it uses MRI, a highly sensitive methodology enabling the detection of subtle and early knee structural changes. In brief, this approach utilized a developed machine learning model that comprised five baseline imaging features: three from MRI (mean cartilage thickness values from central, medial, and peripheral plateaus) and two from X-rays (joint space narrowing [JSN] and joint space width [JSW]. A threshold value that distinguishes structural progressors from non-progressors was subsequently applied.

In the modeling cohort, 91 participants were labeled structural progressors and 61 as non-progressors. The independent dataset used for validation comprised 14 structural progressors and 16 non-progressors. Table I displays the characteristics of the participants.

Dimensionality reduction

To disentangle the highly correlated miRNAs before downstream analyses, we used an unsupervised dimensionality reduction technique that employed the hierarchical clustering variable approach, VarClusHi, implemented in Python.[20] This methodology assessed collinearity and redundancy by organizing variables into clusters that could be aggregated into one variable, thus diminishing the number of variables.[21] This method iteratively breaks down existing variable groups into subgroups until a stopping criterion is fulfilled, providing a straightforward approach for developing scales. Here, we used a cluster-splitting threshold of 0.70, then 0.60, and finally 0.40. Within each cluster, miRNAs were systematically removed based on the highest 1-R2 ratio, engaging in an iterative evaluation of Spearman correlations among the remaining miRNAs. After the third

	Modeling *(serum, n=152)*				Validation *(plasma, n=30)*			
	Progressors[a] (n=91)	Non-progressors (n=61)	Means Difference [95%CI]	p-value[b]	Progressors[a] (n=14)	Non-progressors (n=16)	Means Difference [95%CI]	p-value[b]
Age (years)	64.7 ± 9.1	57.7 ± 8.4	−7.1 [−9.9, −4.2]	**≤0.001**	59.8 ± 10.5	58.8 ± 8.2	−1.0 [−8.0, 6.0]	0.951
OAI cohort				**≤0.001**				0.675
Incidence, % (n)	0 (0)	14.8 (9)			71.4 (10)	81.3 (13)		
Progression, % (n)	100 (91)	85.2 (52)			28.6 (4)	18.8 (3)		
Race				**≤0.001**				0.209
1 Caucasian, % (n)	100 (91)	75.4 (46)			85.7 (12)	100 (16)		
2 African American, % (n)	0 (0)	24.6 (15)			14.3 (2)	0 (0)		
Gender, Male, % (n)	50.5 (46)	37.7 (23)		0.137	42.9 (6)	50.0 (8)		0.730
BMI (kg/m²)	30.0 ± 4.9	29.2 ± 4.7	−2.4 [−2.4, 0.8]	0.626	28.4 ± 4.7	26.7 ± 3.8	−1.7 [−4.8, 1.5]	0.580
WOMAC								
Pain (score 0–20)	5.2 ± 3.2	3.9 ± 3.6	−1.3 [−2.4, −0.2]	**0.008**	2.1 ± 2.1	0.0 ± 0.0	−2.1 [−3.3, −0.8]	**0.001**
Function (0–68)	15.6 ± 9.7	11.2 ± 11.8	−4.4 [−7.8, −0.9]	**0.003**	5.4 ± 6.3	0.1 ± 0.3	−5.3 [−8.9, −1.7]	**0.003**
Stiffness (0–8)	2.6 ± 1.5	2.1 ± 1.6	−0.6 [−1.1, −0.04]	**0.041**	1.4 ± 1.3	0.1 ± 0.3	−1.4 [−2.1, −0.6]	**0.001**
Total (0–96)	23.4 ± 13.1	17.2 ± 15.9	−6.2 [−10.9, −1.6]	**0.002**	8.9 ± 8.5	0.1 ± 0.3	−8.7 [−13.6, −3.8]	**≤0.001**
Kellgren-Lawrence grade, % (n)				**≤0.001**				**0.014**
0	0 (0)	0 (0)			64.3 (9)	100.0 (16)		
1	4.4 (4)	41.0 (25)			35.7 (5)	0.0 (0)		
2	14.3 (13)	55.7 (34)			0.0 (0)	0.0 (0)		
3	46.2 (42)	3.3 (2)			0.0 (0)	0.0 (0)		
4	35.2 (32)	0 (0)			0.0 (0)	0.0 (0)		
JSW (mm)	2.1 ± 1.3	4.4 ± 0.7	2.4 [2.0, 2.7]	**≤0.001**	3.8 ± 0.6	4.6 ± 0.7	0.8 [0.1, 1.4]	**0.046**
JSN score	1.5 ± 0.5	0.1 ± 0.2	−1.4 [−1.6, −1.3]	**≤0.001**	0.9 ± 0.3	0.1 ± 0.3	−0.8 [−1.0, −0.6]	**≤0.001**

Results are mean ± standard deviation (SD) or number (n) and percentage (%) of participants.
BMI, body mass index; CI, confidence interval; JSW, joint space width; JSN, joint space narrowing, score (scoring at baseline was 0-2, as described in the OAI database); WOMAC, Western Ontario and McMaster Universities Osteoarthritis Index.
[a] The classification of structural progressors and non-progressors is detailed in the Methods section.
[b] Continuous variables were analyzed using Student's t-test or the Mann-Whitney test, while proportions were compared using the Chi-squared test or Fisher's exact test. *P values* ≤0.050 (in bold) were considered statistically different.

Table I

Participants baseline characteristics.

Osteoarthritis and Cartilage

iteration, 107 clusters were formed with correlations below 0.40 (Supplementary Table S1A).

One miRNA was selected for each cluster based on the Reduction in the Sum of Squares Ratio (RS Ratio) value, a metric derived from the VarClusHi clustering model to ensure representativeness. The RS Ratio quantitatively measures each miRNA's contribution to the total variance within its respective cluster. The list of the 107 selected miRNAs is provided in Supplementary Table S1B.

Feature selection

In addition to the 107 selected miRNAs, we incorporated four risk factors associated with OA: age, sex, BMI, and race (1, Caucasian and 2, African American). Of note, these factors have also been shown to impact circulating miRNA.[22] Using these 111 features, we aimed to identify the top predictors of knee OA structural progression. This feature selection approach embraced a comprehensive exploration of diverse models, including Decision Tree,[23] Elastic Net,[24] Gradient Boosting Machine,[25] Lasso,[25] Random Forest,[26] Recursive Feature Elimination,[27] and Ridge Regression.[28] Each method underwent rigorous evaluation within a fivefold cross-validation setup, repeated five times for hyperparameter tuning. We selected the best machine learning model based on its performance during cross-validation on the training dataset, leveraging metrics such as AUC, accuracy, sensitivity, and specificity, with their 95% CI. The model was then evaluated on the test dataset, and we further ensured robustness by performing a validation analysis using an independent set of OAI participants.

Feature relative importance and impact

Relative feature importance was calculated using the caret package in R with the varImp function, in which the Relative importance = (Importance - Minimum Importance)/Maximum Importance - Minimum Importance) * 100. The impact of each feature was analyzed using logistic regression.

Machine/deep learning model development

The model development process was characterized by a multifaceted exploration, encompassing an array of machine/deep learning models, including Artificial Neural Network (ANN),[29] Decision Tree,[23] Kernel Support Vector Machine,[30] Penalized Logistic Regression,[25] Random Forest,[26] Ridge Regression,[28] and Support Vector Machine.[31] As mentioned above, each model was evaluated with fivefold cross-validation with five repetitions. AUC, accuracy, sensitivity, specificity and their [95% CI] were assessed to find the best model. We established pre-specified decision rules for model evaluation, where AUC [95% CI] was our primary metric for assessing model performance, with a minimum acceptable threshold of 0.70 for the point estimate. Secondary performance thresholds included a minimum accuracy of 0.75 and balanced performance between sensitivity and specificity (difference < 0.15). To ensure robust estimates of model performance, we used the Agresti-Coull interval[16] for the modeling cohort and the Wilson score interval[17] for the validation cohort to calculate the 95% CI for all accuracy metrics in all models.

The generalizability and robustness of the models were also assessed with a validation dataset (independent to the one used for the modeling) of plasma samples. For model validation assessment, we applied the same decision rules as described above. The optimal model was further evaluated with an internal validation performed with the Monte Carlo cross-validation with 100 simulations to ensure its robustness and stability.

Results

Participants

The post hoc sample size calculation showed that 46 participants per group were required for reliable AUROC estimation. Our dataset of 152 total samples (91 progressors and 61 non-progressors) exceeded this requirement, ensuring sufficient power for model development and minimizing the risk of Type I and Type II errors.

Comparisons of the baseline participants characteristics of the modeling cohort (Table I) showed that the participants in the non-progressor group were younger, the Caucasians were all in the progressor group, and the African Americans were in the non-progressor group. The independent validation dataset (Table I) indicated, among the progressors and the non-progressors, no significant differences in sex, BMI, age, and race. However, both modeling and validation participants significantly differed in the Western Ontario and McMaster Universities Osteoarthritis Index (WOMAC) scores, KL grades, JSW, and JSN measurements. Of note, the average WOMAC scores, KL grades, and JSN were lower in the validation cohort than in the modeling (Table I), potentially because a larger proportion of participants from the OAI progression subcohort was in the modeling cohort versus the validation cohort.

Feature selection

The input for each of the seven screened machine-learning models included the 107 selected miRNAs from the clustering analysis plus four OA risk factors: age, sex, BMI, and race. As represented in Supplementary Table S2, although the Random Forest model exhibited higher AUC and specificity, Elastic Net demonstrated superior accuracy and sensitivity. Elastic Net was preferred due to its better handling of multicollinearity and robust performance in imbalanced datasets, making it the chosen model for feature selection. Using Elastic Net, the ten top features were identified. They consisted of race2 indicator (African American), age, and BMI, plus seven miRNAs: hsa-miR-141-3p, hsa-let-7c-5p, hsa-miR-556-3p, hsa-miR-3667-5p, hsa-miR-3157-5p, hsa-miR-200a-5p, hsa-miR-224-5p. The respective importance of each feature is illustrated in Fig. 2.

Although the race2 indicator had the highest impact on predicting knee OA progressors, we hypothesized that this was driven by the fact that all the African Americans were labeled as non-progressors in this cohort. To further assess this, we investigated whether removing the race2 indicator and BMI (which exhibited very low impact) as inputs affected the model accuracies (Fig. 3). In the receiver operating characteristic (ROC) curves, discrimination thresholds are systematically adjusted to assess the classifier's performance across different operating points, providing insights into its ability to discriminate between the two classes. Fig. 3A illustrates that excluding race2 and/or BMI as inputs did not influence the Elastic Net model's performance. Consequently, these features were excluded from further analysis. Fig. 3B shows the importance of the selected features when race2 and/or BMI are discarded.

Machine/deep learning prediction model development

Seven advanced machine/deep learning-based models were explored to develop the optimal predictive model. The hyperparameters of each model were tuned to enhance their predictive capabilities. We systematically varied the composition of feature subsets, ranging from a minimum of three to all eight selected features (age and seven miRNAs), across all seven models. This thorough exploration resulted in extensive model iterations, as each model was tested with every possible combination of selected features within the specified range. This approach enabled us to

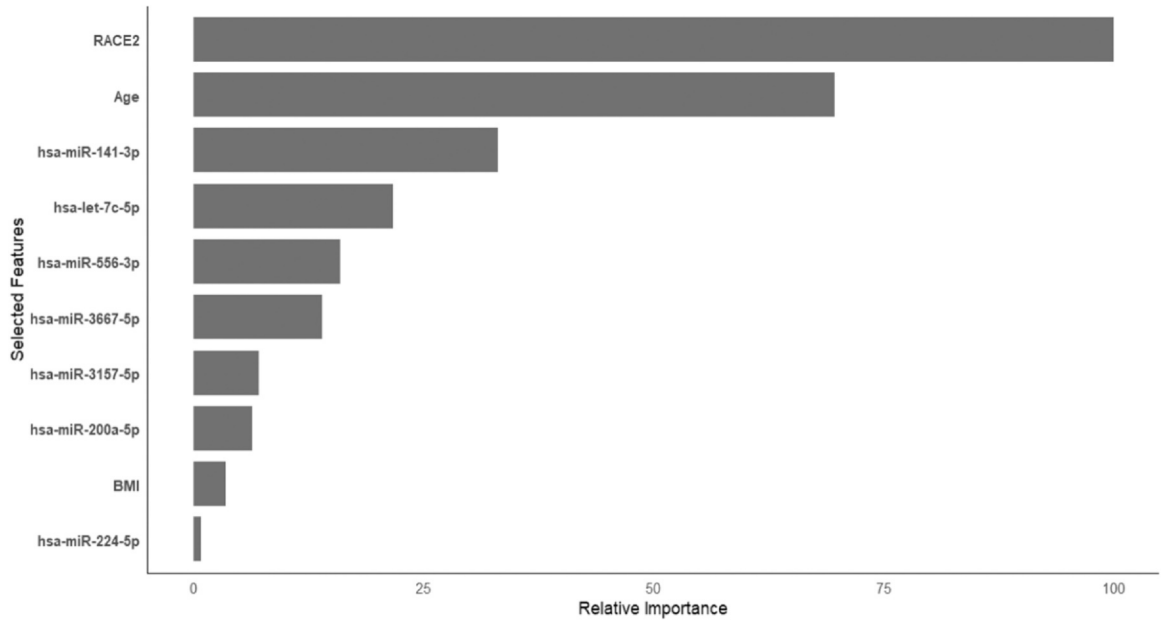

Fig. 2 Osteoarthritis and Cartilage

The relative importance of the top ten selected features using the Elastic Net model. BMI (body mass index); Race2, indicator of African Americans.

identify the most informative features for each model, tailoring the model's input to its specific strengths and characteristics.

The optimal feature combinations for both the modeling and validation cohorts for each machine/deep learning model are presented in Table II. The culmination of our predictive modeling revealed that ANN with five features (age and four miRNAs, hsa-miR-556-3p, hsa-miR-3157-5p, hsa-miR-200a-5p, and hsa-miR-141-3p) achieved the best prediction performance (Fig. 4). In the modeling cohort, we observed an AUC of 0.94 [0.89, 0.97)], which surpasses our primary metric threshold of 0.70 (lower bound), indicating strong generalization potential (Table II). The accuracy was 0.84 [0.77, 0.89], above our secondary threshold of 0.75 (lower bound), while sensitivity and

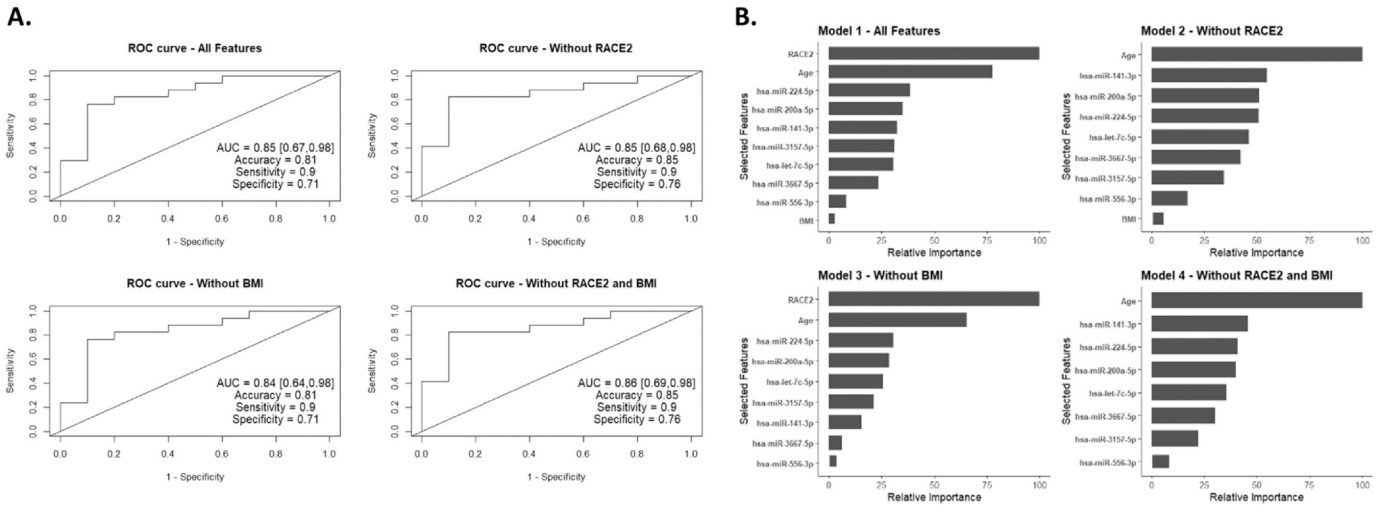

Fig. 3 Osteoarthritis and Cartilage

(A) The ROC curve for Elastic Net models with and/or without race2 and BMI. ROC curves plot sensitivity (true positive rate) on the y-axis against 1-specificity (false positive rate) on the x-axis, with the diagonal indicating random chance. **(B)** Feature relative importance for the Elastic Net models with and/or without race2 and BMI. AUC [], area under the curve [95% confidence interval]; BMI, body mass index; Race2, indicator of African Americans.

Model	Optimal Features	Cohort	AUC [95% CI]	Accuracy [95% CI]	Sensitivity [95% CI]	Specificity [95% CI]
Artificial Neural Network	Age, hsa-miR-556-3p, hsa-miR-141-3p, hsa-miR-3157-5p, and hsa-miR-200a-5p	Modeling	0.94 (0.89, 0.97)	0.84 (0.77, 89)	0.89 (0.81, 0.94)	0.75 (0.63, 0.85)
		Validation	0.81 (0.63, 0.92)	0.83 (0.66, 0.93)	0.71 (0.45, 0.88)	0.94 (0.72, 0.99)
Decision Tree	Age, hsa-miR-556-3p, hsa-miR-200a-5p	Modeling	0.86 (0.80, 0.91)	0.71 (0.63, 0.78)	0.84 (0.75, 0.90)	0.42 (0.31, 0.55)
		Validation	0.57 (0.38, 0.74)	0.71 (0.52, 0.85)	0.84 (0.58, 0.96)	0.50 (0.28, 0.72)
Random Forest	Age, hsa-miR-3667-5p, hsa-let-7c-5p, hsa-miR-3157-5p	Modeling	0.87 (0.81, 0.92)	0.90 (0.84, 0.94)	0.89 (0.81, 0.94)	0.92 (0.82, 0.97)
		Validation	0.68 (0.49, 0.83)	0.70 (0.52, 0.84)	0.57 (0.33, 0.79)	0.81 (0.57, 0.93)
Kernel Support Vector Machine	Age, hsa-miR-141-3p, hsa-miR-224-5p, hsa-let-7c-5p, hsa-miR-200a-5p	Modeling	0.94 (0.89, 0.97)	0.94 (0.89, 0.97)	1.00 (0.96, 1.00)	0.83 (0.72, 0.91)
		Validation	0.78 (0.60, 0.90)	0.53 (0.36, 0.70)	0.00 (0.00, 0.22)	1.00 (0.81, 1.00)
Penalized Logistic Regression	Age, hsa-miR-141-3p, hsa-let-7c-5p, and hsa-miR-200a-5p	Modeling	0.95 (0.90, 0.98)	0.84 (0.77, 0.89)	1.00 (0.96, 1.00)	0.58 (0.46, 0.70)
		Validation	0.67 (0.48, 0.82)	0.60 (0.42, 0.76)	0.43 (0.22, 0.67)	0.75 (0.51, 0.90)
Gradient Boosting Machine	Age, hsa-let-7c-5p, hsa-miR-3157-5p, hsa-miR-200a-5p	Modeling	0.89 (0.83, 0.93)	0.81 (0.74, 0.87)	0.89 (0.81, 0.94)	0.67 (0.55, 0.77)
		Validation	0.76 (0.58, 0.89)	0.70 (0.52, 0.84)	0.79 (0.52, 0.92)	0.62 (0.39, 0.81)
Support Vector Machine	Age, hsa-miR-3667-5p, hsa-miR-141-3p, hsa-let-7c-5p, hsa-miR-3157-5p, hsa-miR-200a-5p	Modeling	0.97 (0.93, 0.99)	0.90 (0.84, 0.94)	0.95 (0.88, 0.98)	0.83 (0.72, 0.91)
		Validation	0.44 (0.27, 0.63)	0.57 (0.39, 0.73)	0.21 (0.08, 0.48)	0.88 (0.64, 0.97)

The best performance of seven models with the optimum features. AUC, area under the curve; CI, confidence interval.

Table II

Model performance comparison of machine/deep learning models.

specificity were 0.89 [0.81, 0.94] and 0.75 [0.63, 0.85], respectively. The lower bound of the specificity fell below 0.70 due to the inherent variability in our training data and the influence of a relatively small sample size of 152 samples, with 20% allocated as test data. This variability can lead to less stable estimates, particularly for specificity, where misclassification of a few samples can significantly impact the overall measure, as noted by the acceptable performance difference of < 0.15.

For the validation cohort, the model yielded an AUC of 0.81 [0.63, 0.92], accuracy of 0.83 [0.66, 0.93], sensitivity of 0.71 [0.45, 0.88], and specificity of 0.94 [0.72, 0.99] (Table 2). Although all maintain an acceptable performance difference, the small sample size contributed to widening the CI. Subsequently, we performed an internal Monte Carlo cross-validation on the final prediction model, utilizing 100 simulations. These data revealed an average AUC of 0.92 [0.86 to 0.97], accuracy of 0.85 [0.77, 0.91], sensitivity of 0.84 [0.76, 0.90], and specificity of 0.88 [0.80, 0.93] (Supplementary Fig. S2).

Additionally, we examined the contribution of each feature to the prediction outcome. As illustrated in Supplementary Fig. S3, our findings reveal distinct effects of these features on the prediction, with some exerting positive influences while other negative. Specifically, age and hsa-miR-3157–5p emerged as positively impacting the likelihood of an individual being predicted as a progressor. Conversely, hsa-miR-556–3p, hsa-miR-200a-5p, and hsa-miR-141–3p were found to have a negative impact on the outcome, thereby decreasing the probability of being a progressor.

The ANN designed using the Keras sequential model comprised an input layer, a hidden layer with five units and ReLU activation, and an output layer with one unit and sigmoid activation. The model was compiled with the Adam optimizer set to a learning rate of 0.001 and binary cross-entropy as the loss function.[32] To address class imbalances in our training data, we utilized the Synthetic Minority Oversampling Technique (SMOTE) implemented via the imbalanced-learn library in Python.[33] SMOTE generates synthetic samples for the minority class, ensuring a more balanced distribution of class labels.[34] By augmenting the representation of the minority class, SMOTE enhanced the robustness of our developed model and improved its generalization capability. Specifically, class weights were adjusted, assigning a weight of 1.3 for non-progressors and 1 for progressors.

Sensitivity analysis

In examining the clusters from the VarClusHi analysis associated with each of the four miRNAs incorporated into an optimally developed ANN model, we observed that all but one miRNA was solitary in their respective clusters. Hsa-miR-141-3p was clustered with one other miRNA, hsa-miR-194-5p (cluster 7, Supplementary Table S1A). This observation prompted a sensitivity analysis to explore the potential impact of including hsa-miR-194-5p as one of the features in the final model. Data showed that the introduction of hsa-miR-194-5p resulted in a notable decrease across all accuracy metrics, in which the average AUC and accuracy consistently remained around 0.56. This decline suggests potential overfitting, given the similarity and collinearity between hsa-miR-194-5p and the already included hsa-miRNA-141-3p in the model. Furthermore, replacing hsa-miR-141-3p with hsa-miR-194-5p in the final model also yielded unsatisfactory results, with both AUC and accuracy decreasing to 0.72 (modeling) and 0.61 (independent validation). These data also support the selection of hsa-miR-141-3p over hsa-miR-194-5p with the

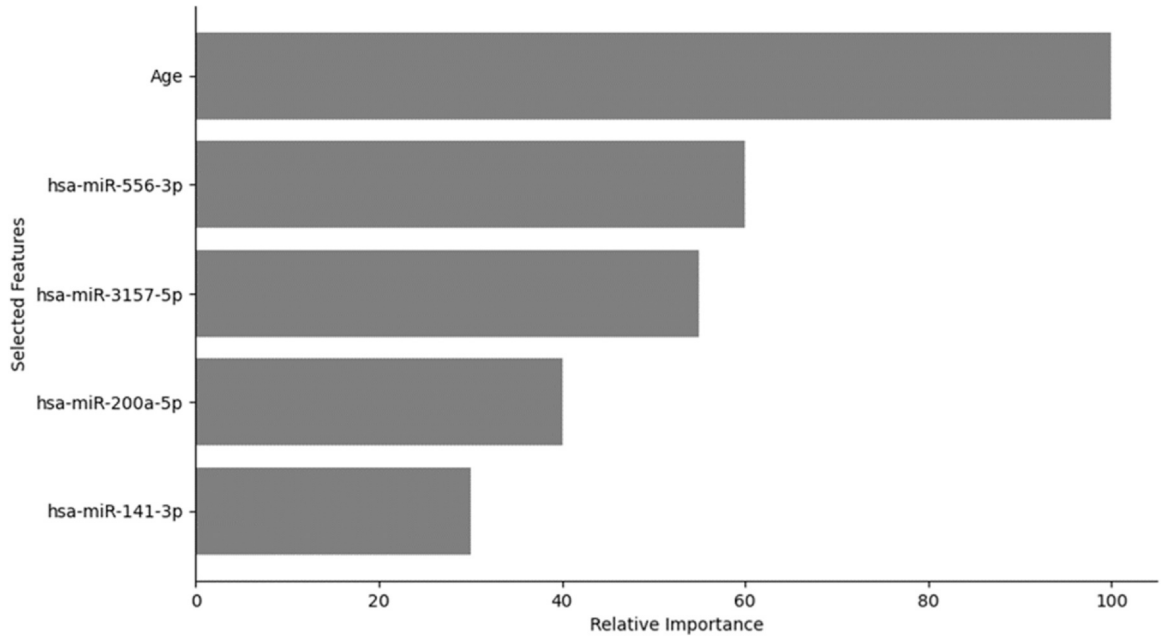

Fig. 4

Osteoarthritis and Cartilage

The relative importance of the five features included in the developed ANN model.

clustering method and underscore the superiority of hsa-miR-141-3p as a candidate for inclusion in the model.

Discussion

This study introduces a novel deep-learning model for predicting knee structural OA progression. To test our hypothesis, we first employed a sensitive imaging-based classification to label OAI participants as progressors and non-progressors. Next, we applied a multi-step feature selection process to identify relevant miRNAs. Finally, through systematic machine/deep learning-based analyses, we developed a miRNA-based prediction model that successfully met our goal of predicting OA structural progressors with a high performance. The model achieved an AUC of 0.94 [0.89, 0.97] using only four miRNAs and age as features. This performance was replicated on a validation cohort, with an AUC of 0.81 [0.63, 0.92], further confirming the model's robustness and generalizability.

In previous work,[19] we developed a prognosis model for OA structural progressors using single nucleotide polymorphism genes and mitochondrial DNA haplogroups as biomarkers. In the present study, we focused on circulating miRNAs due to their high stability in biofluids and their impact on many signaling pathways and cellular processes. Unlike genetic markers, which are static, miRNAs offer a dynamic and real-time perspective of disease states, capturing the intricate and fluctuating regulatory networks that drive pathology.[35] Moreover, contrasting to the prior work[19] in which the genes were selected before the model development, we took an unbiased sequencing approach and investigated 456 miRNAs. Data revealed that four miRNAs, hsa-miR-556–3p, hsa-miR-3157–5p, hsa-miR-200a-5p, and hsa-miR-141–3p, along with age, predicted OA structural progressors with high performance. Whereas data showed that age has the highest relative importance, the model should be used as a whole because using fewer than the five features reduced the performance mainly on the validation cohort (Supplementary Table S3).

In a previous study, several members of the miR-320 family were identified as upregulated in fast-progressing knee OA,[9] though none were determined to be important features within our model. This discrepancy could be due to differences in the definitions of OA progression used by each study. First, the previous study[9] assessed fast-, slow-, and non-OA progressors compared to our binary categorization, meaning we combined fast and slow progressors together. Second, though both studies used imaging to discriminate OA progressors, the previous study was limited to X-ray characteristics, while this present model utilized both X-ray and MRI features.

While three of the miRNAs (hsa-miR-556-3p, hsa-miR-200a-5p, and hsa-miR-141-3p) showed a negative impact on the outcome, thus decreasing the probability of becoming a progressor, only two of them, hsa-miR-141-3p and hsa-miR-556-3p, have been explored in OA pathology. Hsa-miR-141-3p is upregulated in OA chondrocytes and is responsible for increasing apoptosis and cartilage destruction. However, in OA chondrocytes, the target factors differed within studies.[36,37] In OA joints, hsa-miR-141-3p has also been identified in OA fibroblast-like synoviocytes,[38] and has been reported to promote osteoblastogenesis in OA joints.[39] The second miRNA, hsa-miR-556-3p, is upregulated in the plasma of individuals with early-stage radiographic knee OA.[14] This miRNA was shown to target, among others, the protein phosphatase 1B (PPM1B),[40] which is widely distributed in skeletal muscle, playing a role in many signaling pathways (p38, JNK, IKK, and Smad2) involved in OA pathology. It may also regulate OA cartilage ferroptosis.[41]

Although hsa-miR-200a has been studied in the development of mandibular condylar cartilage[42] and osteoblast differentiation[43], these studies did not mention if it was the −3p or −5p arm. However, there is evidence that hsa-miR-200a-5p may regulate lipid metabolism[44], a process altered in OA. Notably, hsa-miR-200a and hsa-miR-141-3p belong to the same family, and although they are located on different chromosomes of the human genome, they share a similar sequence, suggesting similar biological functions.[45,46] Not much is known about hsa-miR-3157-5p, but this miRNA

demonstrated a decrease with age in the plasma of a general prospective health cohort.[47]

Finally, the cluster containing hsa-miR-141-3p is shared with hsa-miR-194-5p, and while they have common targets, they also could have unique direct and indirect targets (Supplementary Fig. S4). While this suggested that hsa-miR-194-5p could be important in the model, the sensitivity analysis supports the selection of hsa-miR-141-3p over hsa-miR-194-5p. Further exploration of these miRNAs and their biological function, especially in OA-related processes, will improve our understanding of this disease pathophysiology.

To address the problem of the high multicollinearity of the miRNAs, we opted to prune the miRNA dataset and select a subset by using a hierarchical clustering method, the VarClusHi methodology. This technique allowed the selection of a representative miRNA from each distinct cluster. While the features were significantly reduced from the original dataset, it still posed a risk of model overfitting and complexity, which could adversely affect performance and interpretability. Therefore, a secondary reduction of the miRNAs was essential. At this step, we included four major OA risk factors to align the feature selection with clinically relevant predictors. To mitigate the risk of feature selection bias, we elected to analyze multiple machine learning methods instead of relying on a single approach, as different machine learning models have unique strengths and biases. Among the models studied, the Elastic Net model was selected due to its inherent design, which combines Lasso and Ridge regularization techniques. Such a combination is particularly effective in handling high collinearity and imbalanced data, two characteristics present in our dataset. These characteristics of Elastic Net ensure that we capture the full range of predictive information, making it more suitable for our study.

In developing our optimal prediction model, we employed seven distinct machine/deep learning methods, and the ANN outperformed the others, particularly in the validation cohort. This can be attributed to its deep learning architecture, which enables it to learn layered representations of the data, making it particularly adept at handling inter-feature interactions. In addition, it can discern intricate patterns within the data, attributes crucial for predictive accuracy in complex biological datasets.

Although one might question the relevance of developing such a prognostic model in the absence of DMOADs, the current model holds promise for precision medicine. It could serve as a decision-support tool for healthcare professionals, enhancing their ability to screen and manage high-risk patients, leading to timely and targeted interventions, thus improving patient outcomes. Furthermore, the model has high clinical relevance in guiding decision-making for future DMOAD studies. At present, the challenges in developing such drugs are due at least in part to the fact that often, in these clinical trials, patients already exhibit significant structural degeneration. Hence, the inability to screen participants based on progression has led to trials with insufficient statistical power to evaluate the effectiveness of the intervention. Our prognostic model could address this challenge by improving the identification of patients at risk of OA progression, thereby lowering trial costs and creating opportunities for testing more interventions.

Among the strengths of this study is the significant positive correlation observed between serum and plasma miRNAs, concurring with previous studies.[11,48] Such data are important as some biochemical parameters demonstrate significant differences when employing serum versus plasma samples.[49,50] This lends to future translation of this miRNA signature as a prognostic tool that can be applied to either serum or plasma in clinical settings, supporting the utility of miRNAs as biomarkers for disease.

A second strength of this study is incorporating an internal cross-validation analysis while systematically exploring multiple model frameworks for the feature selection, modeling, and validation assessment. For the final prediction model, we chose the Monte Carlo technique due to its effectiveness in handling limited and imbalanced datasets, for which traditional n-fold cross-validation approaches would have been inadequate. A third strength, classifying knee OA participants into structural progressors and non-progressors by applying two baseline imaging features, MRI and radiography,[4] offers a more thorough evaluation of knee OA structure. Fourth, we chose to use machine/deep learning approaches instead of statistical analysis for the prediction modeling, as it is well known that while the latter frequently reveals many associations, it lacks predictive significance.[51] Fifth, this model was developed by leveraging high-throughput miRNA-sequencing data, the most comprehensive and unbiased method of quantifying miRNAs currently available. Finally, for two of the miRNAs identified in our predictive model, hsa-miR-200a-5p and hsa-miR-3157-5p, this is the first report of their association with OA.

Among the study's limitations was that participants included Caucasians and African Americans, all from North America, while other ethnic groups from Europe or Asia, for instance, could be studied for broader generalization. Furthermore, although our total sample size of 152 is considered above adequate power for miRNA biomarker discovery,[52] one can argue that it may be limited for machine/deep learning model development. To address the relatively small sample sizes, at the beginning of our analysis, we applied variable clustering to reduce the dimensions of miRNA features from 456 to 107. This technique allowed us to have fewer features than the number of samples (n=152), which helped us avoid overfitting. Moreover, the methodological approaches focusing on maximizing the informativeness of each sample, utilizing feature selection, is particularly effective in small sample sizes as it can handle datasets with a high feature-to-sample ratio, thereby lessening the risk of overfitting. We also conducted a sample size calculation, confirming that the number of samples provided reliable estimates of model performance. In addition, we applied several metrics, such as AUC [95% CI] using the Agresti-Coull interval for the modeling cohort and the Wilson score interval for the validation cohort in all feature selection and prediction model analyses, along with accuracy, sensitivity, specificity and their [95% CI] for all models. As mentioned above, we also implemented Monte Carlo cross-validation with 100 simulations to ensure the robustness and stability of our final prediction model. Finally, the model robustness was further confirmed through the validation cohort, substantiating the generalizability of the developed ANN model.

In conclusion, this study enriches the knowledge of miRNAs in OA and provides a signature for early prognosis of knee structural progression. The signature comprising four circulating miRNAs, hsa-miR-556–3p, hsa-miR-3157–5p, hsa-miR-200a-5p, and hsa-miR-141–3p, combined with age, can distinguish, at an early stage and independent of disease status, individuals likely to develop progressive knee OA. This prognosis model could inform future research by providing insights into factors that may influence disease progression and outcomes, revealing patterns that may not be immediately apparent and thus advancing our understanding of disease pathophysiology. For healthcare professionals, this medical prognosis model for early prediction of OA progressors could allow for more personalized and targeted treatment plans, leading to better outcomes. Moreover, it could also be beneficial for patients, as being better informed may support decision-making and encourage adherence to current interventions. This is especially important if the patient has modifiable risk factors that could impact their outcomes. As mentioned above, this prognosis model will also assist in the development of more effective DMOADs via the recruitment of progressors to clinical trials.

Looking ahead, the next step involves transforming this automated screening model into a comprehensive, user-friendly

application. This will simplify the prognostic process, making it efficient and easy to use for healthcare professionals who encounter OA. Once integrated into clinical workflows, this tool has the potential to enhance personalized patient care by facilitating early intervention and tailored treatment plans based on each patient's unique risk profile.

Ethics

All Osteoarthritis Initiative (OAI) participants provided written informed consent for participation in the OAI. Ethics approval was obtained by each OAI clinical site (University of Maryland Baltimore Institutional Review Board, Ohio State University's Biomedical Sciences Institutional Review Board, University of Pittsburgh Institutional Review Board, and Memorial Hospital of Rhode Island Institutional Review Board) and the OAI coordinating center (Committee on Human Research at the University of California, San Francisco, CA, USA (47–00532). The OAI cohort is described in detail at https://nda.nih.gov/oai.

The Institutional Ethics Committee Board of the University of Montreal Hospital Research Centre (ID-2018–7290, 17.115) approved the project.

Financial support/role of funding source

This work was supported in part by the Osteoarthritis Research Unit of the University of Montreal Hospital Research Centre, the Chair in Osteoarthritis from the University of Montreal, Montreal, Canada, and the Government of Canada's New Frontiers in Research Fund (NFRF) Exploration, awarded to OEG and SAA [NFRFE-2022-00660].

The funders had no role in the study design, data collection, analysis, and interpretation, in the writing of the manuscript, or in the decision to submit it for publication.

Author contributions

All authors were involved in drafting or revising the article and approved publishing the final version. Professors Martel-Pelletier and Ali had full access to all the study's data and took responsibility for the integrity of the data and the accuracy of the data analysis. **Study design and conception.** Martel-Pelletier, Jamshidi, Ali, Espin-Garcia. **Acquisition of data.** Martel-Pelletier, Ali, Jamshidi, Espin-Garcia, Pelletier, Wilson. **Analysis and interpretation of data.** Martel-Pelletier, Jamshidi, Ali, Espin-Garcia, Wilson, Loveless, Pelletier.

Declaration of competing interests

J-P. Pelletier and J. Martel-Pelletier are shareholders in ArthroLab Inc. All the authors have no competing interests to declare about this work.

Data availability

The R and Python codes used in variable clustering, feature selection, and the Artificial Neural Network (ANN) prediction model development are provided at https://github.com/AFSHINJAM/Predict_KOA_with_miRNAs. Data from the OAI cohort used in this study are publicly available at https://data-archive.nimh.nih.gov/oai. The plasma miRNA data employed to validate the model were from an existing OAI dataset deposited to the Gene Expression Omnibus database (accession number GSE183188). All other raw data reported in this study are available upon reasonable request to the corresponding author.

Acknowledgements

The authors would like to thank the Osteoarthritis Initiative (OAI) participants and the Coordinating Center for their work in generating clinical and radiological data of the OAI cohort and for making them publicly available. The OAI is a public-private partnership comprised of five contracts (N01-AR-2-2258; N01-AR-2-2259; N01-AR-2-2260; N01-AR-2-2261; N01-AR-2-2262) funded by the National Institutes of Health (NIH), a branch of the Department of Health and Human Services, and conducted by the OAI Study Investigators. Private funding partners include Merck Research Laboratories, Novartis Pharmaceuticals Corporation, GlaxoSmithKline, and Pfizer Inc. Private sector funding for the OAI is managed by the Foundation for the National Institute of Health (NIH). This manuscript was prepared using an OAI public use data set and does not necessarily reflect the opinions or views of the OAI investigators, the NIH, or the private funding partners.

Also, thanks to ArthroLab Inc. for providing the magnetic resonance imaging data for this study.

Appendix A. Supporting information

Supplementary data associated with this article can be found in the online version at doi:10.1016/j.joca.2024.11.008.

References

1. Li X, Roemer FW, Cicuttini F, MacKay JW, Turmezei T, Link TM. Early knee OA definition-what do we know at this stage? An imaging perspective. Ther Adv Musculoskelet Dis 2023;15, 1759720X231158204.
2. Hannan MT, Felson DT, Pincus T. Analysis of the discordance between radiographic changes and knee pain in osteoarthritis of the knee. J Rheumatol 2000;27:1513–7.
3. Pelletier JP, Cooper C, Peterfy C, Reginster JY, Brandi ML, Bruyere O, *et al.* What is the predictive value of MRI for the occurrence of knee replacement surgery in knee osteoarthritis? Ann Rheum Dis 2013;72:1594–604.
4. Jamshidi A, Leclercq M, Labbe A, Pelletier JP, Abram F, Droit A, *et al.* Identification of the most important features of knee osteoarthritis structural progressors using machine learning methods. Ther Adv Musculoskelet Dis 2020;12:1–12.
5. Ali SA, Peffers MJ, Ormseth MJ, Jurisica I, Kapoor M. The non-coding RNA interactome in joint health and disease. Nat Rev Rheumatol 2021;17:692–705.
6. Mirzamohammadi F, Papaioannou G, Kobayashi T. MicroRNAs in cartilage development, homeostasis, and disease. Curr Osteoporos Rep 2014;12:410–9.
7. Balaskas P, Clegg PD, Fang Y, Cremers A, Smagul A, Welting TJ, *et al.* MicroRNA signatures in cartilage ageing and osteoarthritis. Biomedicines 2023;11:1189.
8. Rocha FAC, Ali SA. Soluble biomarkers in osteoarthritis in 2022: year in review. Osteoarthritis Cartilage 2023;31:167–76.
9. Ali SA, Espin-Garcia O, Wong AK, Potla P, Pastrello C, McIntyre M, *et al.* Circulating microRNAs differentiate fast-progressing from slow-progressing and non-progressing knee osteoarthritis in the Osteoarthritis Initiative cohort. Ther Adv Musculoskelet Dis 2022;14, 1759720X221082917.
10. Peterfy CG, Schneider E, Nevitt M. The osteoarthritis initiative: report on the design rationale for the magnetic resonance imaging protocol for the knee. Osteoarthritis Cartilage 2008;16:1433–41.
11. Wang K, Yuan Y, Cho JH, McClarty S, Baxter D, Galas DJ. Comparing the MicroRNA spectrum between serum and plasma. PLoS One 2012;7, e41561.
12. Hanley JA, McNeil BJ. The meaning and use of the area under a receiver operating characteristic (ROC) curve. Radiology 1982;143:29–36.

13. Buermans HP, Ariyurek Y, van Ommen G, den Dunnen JT, 't Hoen PA. New methods for next generation sequencing based microRNA expression profiling. BMC Genomics 2010;11:716.
14. Ali SA, Gandhi R, Potla P, Keshavarzi S, Espin-Garcia O, Shestopaloff K, *et al*. Sequencing identifies a distinct signature of circulating microRNAs in early radiographic knee osteoarthritis. Osteoarthritis Cartilage 2020;28:1471–81.
15. Potla P, Ali SA, Kapoor M. A bioinformatics approach to microRNA-sequencing analysis. Osteoarthr Cartil Open 2021;3, 100131.
16. Agresti A, Coull BA. Approximate is better than "exact" for interval estimation of binomial proportions. Am Stat 1998;52:119–26.
17. Brown LDC, T. T, DasGupta A. Interval estimation for binomial proportion. Stat Sci 2001;16:101–33.
18. Shan G. Monte Carlo cross-validation for a study with binary outcome and limited sample size. BMC Med Inform Decis Mak 2022;22:270.
19. Bonakdari H, Pelletier JP, Blanco F, Rego-Perez I, Duran-Sotuela A, Jamshidi A, *et al*. Single nucleotide polymorphism genes and mitochondrial DNA haplogroups as biomarkers for early prediction of knee osteoarthritis structural progressors: use of supervised machine learning classifiers. BMC Med 2022;20:316.
20. Jing T. VarClusHi. GitHub; 2019 ⟨https://github.com/jingtt/varclushi⟩.
21. SAS/STAT 15.1 User's Guide. Cary, NC: SAS Institute Inc; 2018. Available: https://support.sas.com/documentation/onlinedoc/stat/151/stathpug.pdf. [Accessed December 5, 2024].
22. Ameling S, Kacprowski T, Chilukoti RK, Malsch C, Liebscher V, Suhre K, *et al*. Associations of circulating plasma microRNAs with age, body mass index and sex in a population-based study. BMC Med Genomics 2015;8:61.
23. Silva MDB, de Oliveira RVC, da Silveira Barroso Alves D, Melo ECP. Predicting risk of early discontinuation of exclusive breastfeeding at a Brazilian referral hospital for high-risk neonates and infants: a decision-tree analysis. Int Breastfeed J 2021;16:2.
24. Zou H, Hastie T. Regularization and variable selection via the elastic net. J Royal Stat Soc 2005;67:301–20.
25. Tibshirani R. Regression shrinkage and selection via the lasso. J Royal Stat Soc 1996;58:267–88.
26. Breiman L. Random forests. Mach Learn 2001;45:5–32.
27. Guyon I, Weston J, Barnhill S, Vapnik V. Gene selection for cancer classification using support vector machines. Mach Learn 2002;46:389–422.
28. Hastie T. Ridge regularization: an essential concept in data science. Technometrics 2020;62:426–33.
29. LeCun Y, Bengio Y, Hinton G. Deep learning. Nature 2015;521:436–44.
30. Schölkopf B, Smola AJ, Müller K-R. Kernel principal component analysis. In: Schölkopf B, Burges CJC, Smola AJ, editors. Advances in Kernel Methods—Support Vector Learning. Cambridge, MA, USA: MIT Press; 1999. p. 327–52.
31. Bonakdari H, Jamshidi A, Pelletier JP, Abram F, Tardif G, Martel-Pelletier J. A warning machine learning algorithm for early knee osteoarthritis structural progressor patient screening. Ther Adv Musculoskel Dis 2021;13:1–16.
32. Kingma D, Ba J. Adam: A method for stochastic optimization. ArXiv; 2014 ⟨https://arxiv.org/abs/1412.6980⟩.
33. Lemaître G, Nogueira F, Aridas CK. Imbalanced-learn: a python toolbox to tackle the curse of imbalanced datasets in machine learning. J Mach Learn Res 2017;18:1–5.
34. Fernandez A, Garcia S, Herrera FJ, Chawla NV. SMOTE for learning from imbalanced data: progress and challenges, marking the 15-year anniversary. J Artif Intell Res 2018;61:863–905.
35. Ardekani AM, Naeini MM. The role of microRNAs in human diseases. Avicenna J Med Biotechnol 2010;2:161–79.
36. Park S, Oh J, Kim YI, Choe SK, Chun CH, Jin EJ. Suppression of ABCD2 dysregulates lipid metabolism via dysregulation of miR-141:ACSL4 in human osteoarthritis. Cell Biochem Funct 2018;36:366–76.
37. Yang Q, Li X, Zhou Y, Fu W, Wang J, Wei Q. A LINC00341-mediated regulatory pathway supports chondrocyte survival and may prevent osteoarthritis progression. J Cell Biochem 2019;120:10812–20.
38. Chen YJ, Chang WA, Wu LY, Huang CF, Chen CH, Kuo PL. Identification of novel genes in osteoarthritic fibroblast-like synoviocytes using next-generation sequencing and bioinformatics approaches. Int J Med Sci 2019;16:1057–71.
39. Yu X-M, Meng H-Y, Yuan X-L, Wang Y, Guo Q-Y, Peng J, *et al*. MicroRNAs' involvement in osteoarthritis and the prospects for treatments. Evid Based Complement Alternat Med 2015;2015, 236179.
40. Li Z, Chen R, Li Y, Zhou Q, Zhao H, Zeng K, *et al*. A comprehensive overview of PPM1B: from biological functions to diseases. Eur J Pharmacol 2023;947, 175633.
41. Qiu Y, Yao J, Li L, Xiao M, Meng J, Huang X, *et al*. Machine learning identifies ferroptosis-related genes as potential diagnostic biomarkers for osteoarthritis. Front Endocrinol 2023;14, 1198763.
42. Umeda M, Terao F, Miyazaki K, Yoshizaki K, Takahashi I. MicroRNA-200a regulates the development of mandibular condylar cartilage. J Dent Res 2015;94:795–802.
43. Itoh T, Nozawa Y, Akao Y. MicroRNA-141 and -200a are involved in bone morphogenetic protein-2-induced mouse pre-osteoblast differentiation by targeting distal-less homeobox 5. J Biol Chem 2009;284:19272–9.
44. Elkhawaga SY, Ismail A, Elsakka EGE, Doghish AS, Elkady MA, El-Mahdy HA. miRNAs as cornerstones in adipogenesis and obesity. Life Sci 2023;315, 121382.
45. Belgardt BF, Ahmed K, Spranger M, Latreille M, Denzler R, Kondratiuk N, *et al*. The microRNA-200 family regulates pancreatic beta cell survival in type 2 diabetes. Nat Med 2015;21:619–27.
46. Kim YK, Wee G, Park J, Kim J, Baek D, Kim JS, *et al*. TALEN-based knockout library for human microRNAs. Nat Struct Mol Biol 2013;20:1458–64.
47. Freedman JE, Gerstein M, Mick E, Rozowsky J, Levy D, Kitchen R, *et al*. Diverse human extracellular RNAs are widely detected in human plasma. Nat Commun 2016;7, 11106.
48. Malakootian M, Gholipour A, Oveisee M. Comprehensive bioinformatics analysis of key miRNAs and signaling pathways in the body fluids of human knee osteoarthritis. Cell Mol Biol 2023;69:88–97.
49. Quinlivan EP, Crider KS, Zhu JH, Maneval DR, Hao L, Li Z, *et al*. Hypomethylation of serum blood clot DNA, but not plasma EDTA-blood cell pellet DNA, from vitamin B12-deficient subjects. PLoS One 2013;8, e65241.
50. Jonsson A, Hjalmarsson C, Falk P, Ivarsson ML. Levels of matrix metalloproteinases differ in plasma and serum – aspects regarding analysis of biological markers in cancer. Br J Cancer 2016;115:703–6.
51. Poldrack RA, Huckins G, Varoquaux G. Establishment of best practices for evidence for prediction: a review. JAMA Psychiatry 2020;77:534–40.
52. Kok MGM, de Ronde MWJ, Moerland PD, Ruijter JM, Creemers EE, Pinto-Sietsma SJ. Small sample sizes in high-throughput miRNA screens: a common pitfall for the identification of miRNA biomarkers. Biomol Detect Quantif 2018;15:1–5.